

Operation of Gemini Target Area 2 at 5 Hz repetition rate

*Contact: dan.symes@stfc.ac.uk

D. R. Symes*, N. Bourgeois, P. Brummit, O. Chekhlov, C. D. Gregory, S. J. Hawkes, C. J. Hooker, V. Marshall, B. Parry, P. P. Rajeev, E. Springate, Y. Tang, C. Thornton
Central Laser Facility, STFC Rutherford Appleton Laboratory, Didcot OX11 0QX, UK

S. J. D. Dann, J. D. E. Scott, M. J. V. Streeter
The Cockcroft Institute, Keckwick Lane, Daresbury, WA4 4AD, UK

C. D. Baird, C. D. Murphy
York Plasma Institute, Department of Physics, University of York, York YO10 5DQ, UK

S. Eardley, R. A. Smith
Blackett Laboratory, Imperial College London, London SW7 2AZ, UK

S. Rozario, J.-N. Gruse, S. P. D. Mangles, Z. Najmudin
The John Adams Institute for Accelerator Science, Imperial College London, London, SW7 2AZ, UK

1 Introduction

The first two amplifiers of the Gemini laser system (pulse energy up to the Joule-level) operate at 10 Hz before being split into two alternating 5 Hz beams, which separately feed into TA2 and TA3. While the repetition rate of the Quantel pump lasers in the final Gemini amplifier limits TA3 operations to 0.05 Hz, TA2 can be operated at 5 Hz. Until now TA2 has reduced the repetition rate to a maximum of 1 Hz because of the practical challenges of increasing to the full capability. In this report we address these issues and describe the first experimental campaign conducted with the full 5 Hz repetition rate. Furthermore, this allowed us to employ active feedback routines [1] to directly optimize experimental parameters using controllable elements in the laser system.

2 Experimental layout

A schematic diagram of the experiment is shown in fig. 1. The pre-interaction beam was diagnosed with pre-compressor leakage beam near field and far field cameras, a near field camera and wavefront sensor in a leakage beam before the parabola, and a *Grenouille* (Swamp Optics) and spectrometer in a short pulse beam through a hole in the final compressor turning mirror. The laser was focused with an $f/17$ parabola into a 3mm Parker series gas jet. The target was housed within an internal chamber comprising an ISO-160 six-way cross pumped

S. Tata, M. Krishnamurthy
Tata Institute of Fundamental Research, Homi Bhabha Road, Colaba, India

S. V. Rahul
TIFR Centre for Interdisciplinary Sciences, Hyderabad 500 107, India

D. Hazra
Laser Plasma Section, Raja Ramanna Centre for Advanced Technology, Indore 452013, India

P. Pourmoussavi, J. Osterhoff
Deutsches Elektronen-Synchrotron DESY, Notkestr. 85, 22607 Hamburg, Germany

J. Hah, A. G. R. Thomas
Center for Ultrafast Optical Science, University of Michigan, Ann Arbor, Michigan 48109-2099, USA

directly with a large Edwards *iGX* dry pump. The laser entered and exited this cross through 2 mm apertures so that a good vacuum level (below 10^{-4} mbar) was maintained in the main target chamber and the compressor. The post-interaction laser beam was directed to a far field camera and spectrometer. Electron beams generated in the plasma passed a hole in the collection optic and entered a lead shielded enclosure through a 25 mm hole and were diagnosed with a permanent magnet electron spectrometer. Forward directed betatron x-ray emission was measured with a direct detection CCD camera (Andor). Isotropic x-ray plasma emission was measured with x-ray pin diodes mounted on the internal chamber at 90 degrees to the beam axis.

3 Laser pulse shaping

Control of the temporal and spatial properties of the laser pulse were achieved with an acousto-optic programmable dispersive filter (Fastlite *Dazzler*) and an adaptive optic (AO) respectively. The *Dazzler* is integrated in the front end of Gemini and can be used independently of the TA3 pulse to change the spectral phase of the TA2 pulse. The AO was located after the compressor and commissioned during this period. Piezoelectric actuators were used to enable the fast response required for the feedback routine. After acquiring the interaction matrix using CASAO software (Imagine Op-

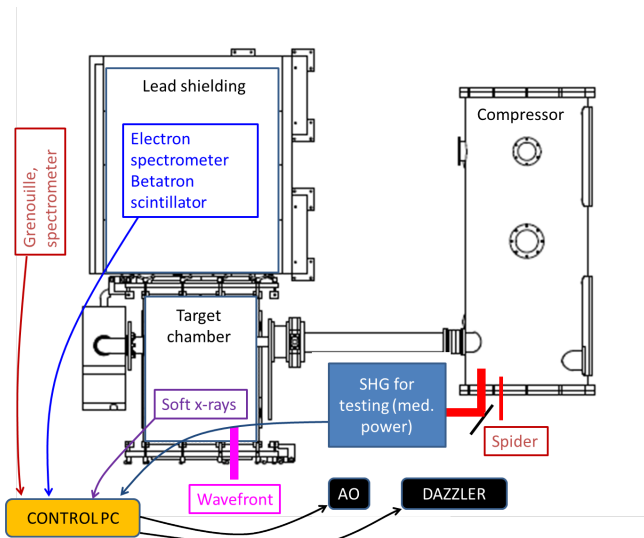


Figure 1: Layout for operating TA2 at high repetition rate. The gas jet is housed in an internal chamber directly connected to an Edwards *iGX* vacuum pump. Data from diagnostics are fed into a control code that can manipulate the pulse properties using the AO and *Dazzler* to improve experimental performance.

tic) a Nelder-Mead algorithm was used to optimize the laser focus by maximizing the energy within a specified region of interest. The improvement of the focus from a nominally flat mirror position to the best focus settings can be seen in fig. 2. This code was subsequently used to apply variable patterns for the optimization routine.

4 High repetition rate control code

To operate at 5Hz and to implement active feedback, the TA2 control code was adapted to provide 50 shot bursts on demand. An extra code was written to run the data acquisition and optimization routine. After each burst this code collected data from the experimental diagnostics and calculated the value of a specified goal function before applying new settings to the controllable element and requesting the next burst. This process was repeated using an algorithm to select the best performing settings to converge towards an optimized laser pulse shape that maximized the goal function. The feedback method was initially trialed by measuring second harmonic signal from a BBO crystal which, as expected, resulted in the shortest pulse and best focus. We then applied it to the control of electron beam energy spectra [2] and x-ray emission from argon atomic clusters [3].

5 Managing the gas load

The internal chamber was connected to the *iGX* vacuum pump positioned adjacent to the main target chamber with large bore ISO-100 fittings to ensure the best

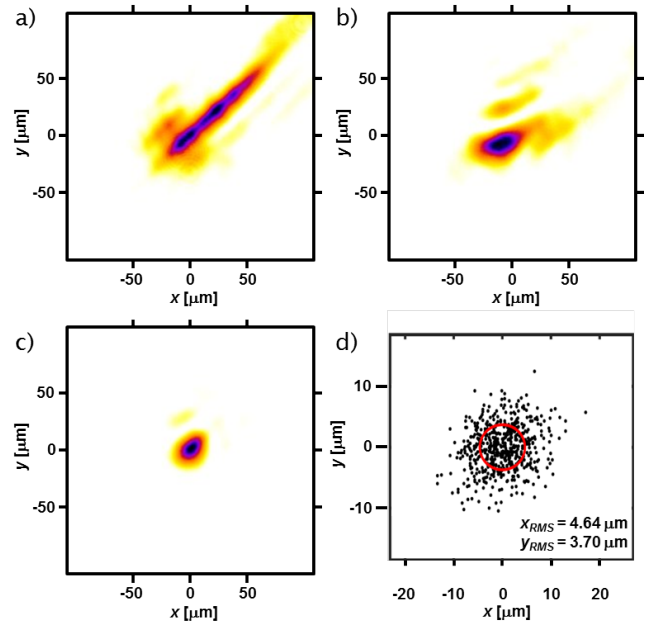


Figure 2: The shape of the focal spot a) before, b) during, and c) after optimization. Each image is separately normalized. The optimization routine started with zero applied voltage (a nominally flat mirror) and maximized the sum of the squares of the counts. Also shown is d) the pre-compressor pointing stability, with the beam size overlaid in red.

throughput. We chose a Parker solenoid because it can operate with very short opening times of order milliseconds. Because we wanted clusters as an interaction target we used a previous characterization [4] to determine the minimum acceptable opening time of ~ 2 ms and the backing pressure required of up to 40 bar. When the jet is operated at high repetition rate a balance is reached at a constant vacuum pressure depending on gas load. We tested this by operating the jet with 1 bar of air (open to the atmosphere) with rates up to 100 Hz. We assumed that these results could be used to estimate the vacuum pressure with equivalent loads at higher pressures (i.e. 1 bar at 100 Hz = 20 bar at 5 Hz). The vacuum pressure is plotted as a function of repetition rate for opening times of 2 ms, 6ms and 10ms in fig. 3.

6 High repetition rate laser performance

At 5 Hz the high average fluence on the compressor gratings is a concern. As a precaution, we carried out daily RF cleaning of the first grating that receives the highest intensity beam. We monitored the throughput by measuring the pre- and post-compression laser energy with the integrated near field signals in the leakage beams. The laser energy showed good stability with 3% standard deviation, excluding 0.6% of laser pulses which had energy less than half the mean. The pre-

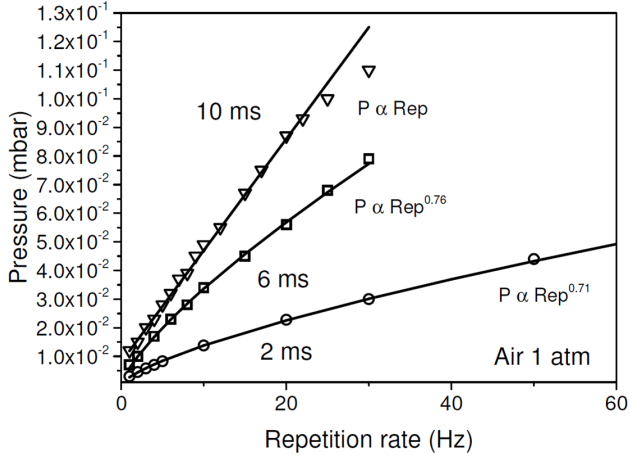


Figure 3: Steady-state pressure inside the internal chamber, for various gas jet opening times and repetition rates, while the gas jet was connected to 1 bar air.

and post-compression signals and their ratio for a data run of 4950 shots (17 minutes) is displayed in (fig. 4a)). There is no drop in the ratio between the two signals indicating a constant compressor throughput (This value is uncalibrated so does not provide an absolute value for compressor throughput but shows any change relative to the starting value.) We also used the pre-compressor far field camera to assess the pointing stability of the beam, shown in fig. 2d), to be $< 5\mu\text{m}$ RMS ($\sim 1/5$ spot size). When the second order term (chirp) of the *Dazzler* was scanned we found that the integrated near field signals increased before the compressor and decreased after it, shown in fig. 4b). This can also be seen in fig. 4c) measured during an optimisation run when the *Dazzler* settings were altered for each data point. While the throughput remains constant, the variation in signal is higher than in fig. 4a). We suspect this effect is caused by a slight change in reflectivity of the mirrors as the spectral phase is changed and these data highlight that care must be taken when using leakage beams as diagnostics when laser parameters are being scanned.

During 5 Hz operation, the post-compression laser pulse slowly becomes longer. This can be seen in fig. 5, which shows the RMS autocorrelation length and the second-order spectral phase, as measured by a *Grenouille*. Since the *Dazzler* settings were kept constant during this time, this appears to be an effect in the compressor. It may be caused by the laser pulses heating the compressor gratings and slightly changing the compressor geometry. In addition, breaks from firing appear to reverse the effect and shorten the laser pulses again, supporting the idea that it is a thermal effect.

In the course of this campaign we delivered $\sim 100,000$ shots to target with no apparent reduction in laser performance. We inspected the optics in the target chamber and found that the silver coating of the parabola was de-

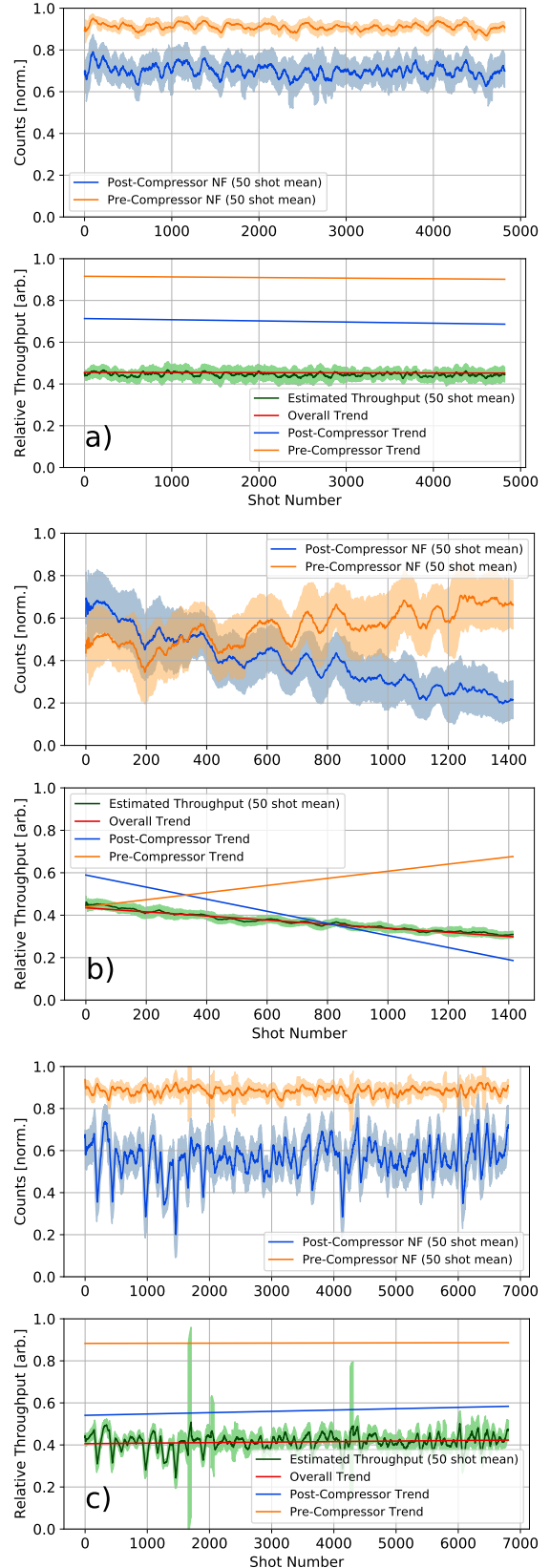


Figure 4: Relative throughput for a) Pressure scan with constant *Dazzler* settings; b) *Dazzler* scan with constant pressure; c) optimisation run with variable *Dazzler* settings.

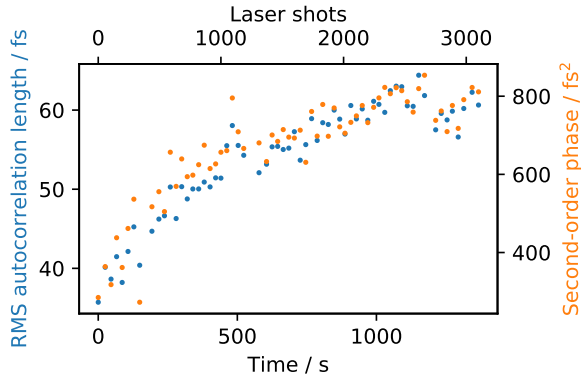


Figure 5: Autocorrelation length and second-order spectral phase, measured by a *Grenouille* while firing the laser and keeping the *Dazzler* settings constant. The average repetition rate is less than 5 Hz due to time taken for data acquisition.

graded significantly (fig. 6a)). This optic had been in use for a long time previously on TA2 experiments and also silver damage thresholds are lower than dielectric mirrors. The dielectric mirror shown in fig. 6b) acted as a fold-mirror in the $f/17$ beamline and received a fluence of 35 mJ cm^{-2} (intensity $7 \times 10^{11} \text{ W cm}^{-2}$). This is well below the manufacturer’s quoted damage threshold and while the beam footprint is visible, the reflectivity of the coating was maintained.

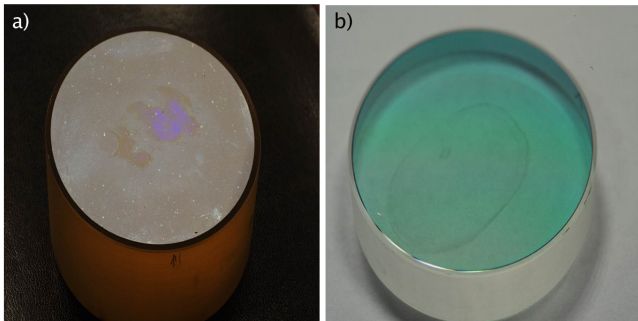


Figure 6: a) Damage to the silver coating of the parabola and b) discolouration of the dielectric coating of a fold-mirror. In the latter case, the reflectivity of the coating was maintained.

7 Safe operations at high repetition rate

Increasing the shot rate to 5 Hz brings additional concerns in terms of possible equipment damage and safety of personnel. We implemented certain measures to ensure safe operations and consider other options that could be implemented in the future both for TA2 and for higher power high repetition rate systems. The principle of the safety system is represented in fig. 7. Several events are identified on the left that would trigger

an alert. Remedial action can take place first on a fast timescale to immediately remove the hazard by stopping the trigger to the gas jet and by inserting a fast shutter ($< 100 \text{ ms}$) into the laser beam. On a slower timescale (several seconds) wall shutters, gate valves and gas system solenoid switches that are already installed in TA2 can be used to cease operations until the situation is deemed to be safe.

Excess gas would suddenly enter the internal chamber if either the *iGX* vacuum pump failed or the high pressure gas jet jammed open. A solenoid valve linked to a pressure switch on the internal chamber was included in the gas supply line as near as possible to the chamber to minimize the residual gas after closure. If the main chamber pressure increased, gate valves would activate to protect the turbomolecular pumps and to isolate the compressor. A 5V signal split from the gate valve signal was installed to operate the fast shutter in LA2. This prevented the high power laser propagating through the compressor gate valve and causing damage to the target chamber optics because of the high B -integral at high repetition rate.

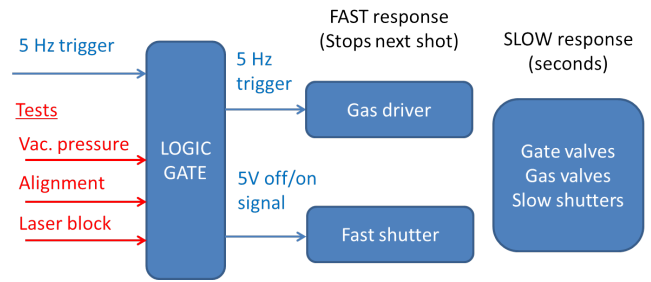


Figure 7: A high-level overview of the proposed machine protection system.

Radiological safety is the greatest hazard with the increase in repetition rate. The radiation escaping from the shielding box through the entrance hole leads to an accumulated dose that must be kept below legal limits. Currently this restricts the maximum number of shots allowed during the campaign but the shielding arrangement could be redesigned to mitigate this problem. More worrying is that a misalignment of the electron beam can mean that it misses the hole completely and dumps against the wall of the vacuum chamber. In this case the radiation quickly surpasses allowable levels. For this reason we placed a Lanex scintillator screen around the hole so that we could immediately see if the electron beam was not centered. This can be seen in fig. 8 where we show in c) the Lanex screen for shots when the laser focus had a slight pulse tilt (fig. 8a)) shifting the electron beam off-axis. After fixing the tilt (diagnosed by removing elongation in the focal spot, fig. 8b)) no bright signal is seen (fig. 8d)), indicating that the electron beam is directed into the hole. In the future, safety measures could be put in place that shutter the laser beam as soon

as an alignment drift outside set tolerances is observed. The feedback signal could derive directly from the electron pointing on the Lanex screen or from the laser beam pointing references.

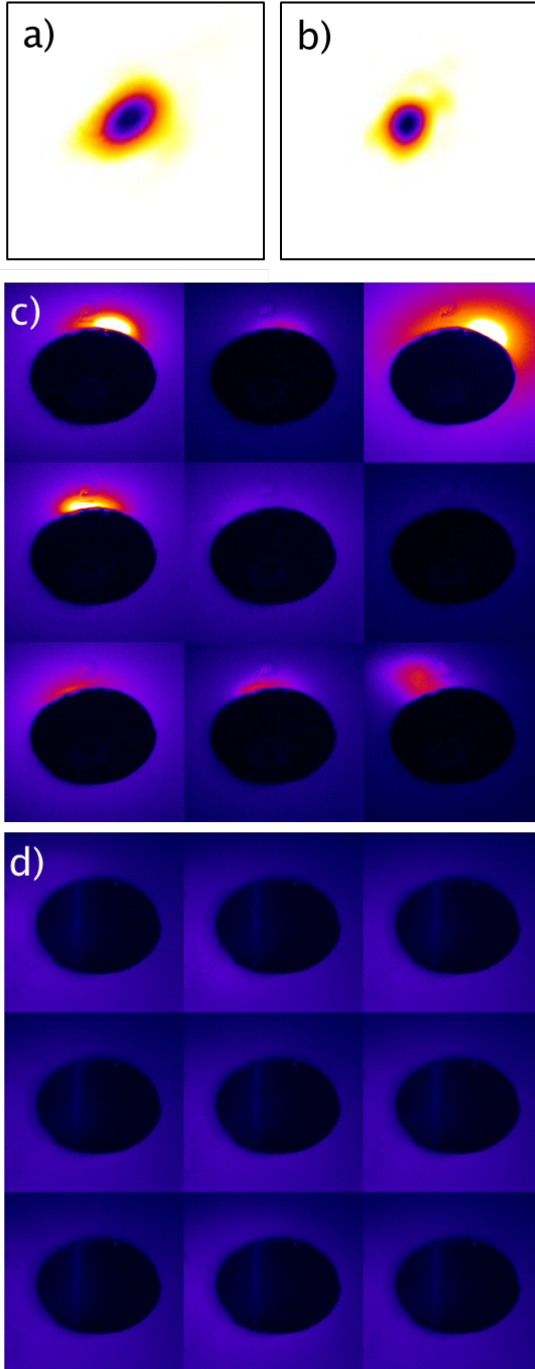


Figure 8: Pulse front tilt can be seen in a) the focal spot and affects the electron beam pointing, causing it to miss c) the pipe leading into the shielded chamber. Removing the pulse front tilt fixes both b) the focal spot and d) the electron beam pointing.

8 Conclusion

In summary, we operated Target Area 2 at the full repetition rate of 5 Hz for the first time delivering about 100,000 shots to target. Changes to the control and safety systems need to be formalised before offering this capability to facility users. Furthermore, radiation shielding and gas handling need to be considered on a case by case basis. With the higher repetition rate we have shown the implementation of active feedback techniques that can be used to explore parameter spaces more effectively than scanning of individual variables [2, 3].

Acknowledgements

We acknowledge funding from STFC (grant numbers ST/P002056/1 and ST/P002021/1), and the EuroNNAc, Newton-Bhabha and Helmholtz ARD programs. SE is supported by an AWE CASE award. JH, JN, KK and AT acknowledge funding from the NSF grant 1535628 and DOE grant DE-SC0016804. The authors also thank the staff of the Central Laser Facility for their expertise and their essential contributions to this work.

References

- [1] W. S. Warren, H. Rabitz, and M. Dahleh. Coherent control of quantum dynamics: the dream is alive. *eng. Science (New York, N.Y.)* **259**, 5101 (Mar. 1993), pp. 1581–1589. URL: <http://www.ncbi.nlm.nih.gov/pubmed/17733021>.
- [2] S. J. D. Dann et al. Laser wakefield acceleration with active feedback at 5 Hz. *In preparation for submission* (2018).
- [3] M. J. V. Streeter et al. Temporal feedback control of high-intensity laser pulses to optimize ultrafast heating of atomic clusters. *arXiv.org* (Apr. 2018). URL: <http://arxiv.org/abs/1804.07488>.
- [4] R. A. Smith, T. Ditmire, and J. W. G. Tisch. Characterization of a cryogenically cooled high-pressure gas jet for laser/cluster interaction experiments. *Review of Scientific Instruments* **69**, 11 (Nov. 1998), p. 3798. URL: <https://aip.scitation.org/doi/abs/10.1063/1.1149181>.